

Time reversibility of a Lamb wave for damage detection in a metallic plate

This article has been downloaded from IOPscience. Please scroll down to see the full text article.

2011 Smart Mater. Struct. 20 025001

(<http://iopscience.iop.org/0964-1726/20/2/025001>)

View [the table of contents for this issue](#), or go to the [journal homepage](#) for more

Download details:

IP Address: 59.162.23.4

The article was downloaded on 09/01/2011 at 12:50

Please note that [terms and conditions apply](#).

Time reversibility of a Lamb wave for damage detection in a metallic plate

B Poddar, A Kumar, M Mitra¹ and P M Mujumdar

Department of Aerospace Engineering, Indian Institute of Technology Bombay, Mumbai 400076, India

E-mail: mira@aero.iitb.ac.in

Received 15 August 2010, in final form 3 December 2010

Published 6 January 2011

Online at stacks.iop.org/SMS/20/025001

Abstract

In this paper, an experimental study has been carried out to develop a baseline-free damage detection technique using the time reversibility of a Lamb wave. The experiments have been carried out on a metallic plate. Time reversibility is the process in which a response signal recorded at a receiver location is reversed in time and transmitted back through the receiver to the original transmitter location. In the absence of any defect or damage in the path between the transmitter–receiver locations, theoretically the signal received back at the original transmitter location (reconstructed signal) is identical to the original input signal. The initial part of the present work is aimed at understanding the time reversibility of a Lamb wave in an undamaged metallic plate. This involves a thorough study of different parameters such as frequency, pulse frequency band width, transducer size and the effects of tuning these parameters on the quality of a reconstructed input signal. This paper also suggests a method to mitigate the effects of the frequency dependent attenuation of Lamb wave modes (amplitude dispersion) and thus achieve better reconstruction for an undamaged plate. Finally, the time reversal process (TRP) is used to detect damage in an aluminium plate without using any information from the undamaged structure. A block mass, a notch and an area of surface erosion are considered as representative of different types of damage. The results obtained show that the effect of damage on TRP is significant, contrary to the results reported earlier.

1. Introduction

In recent years, structural health monitoring (SHM) has attracted a lot of attention from researchers due to its relevance to the safe service of aircraft [1, 2]. Many conventional methods are available for damage detection, but these methods are relatively expensive and require heavy instruments. Thus it is difficult for these methods to be considered for widespread deployment on aircraft structures as part of an SHM system, especially in an *in situ* online mode. Guided waves are of enormous interest in this regard for non-destructive testing of thin walled structures. In these methods information about damage is monitored by changes in characteristics of an elastic wave due to its interaction with the damage, which is recorded by transducers. Lamb waves are the most common form of such elastic waves used for damage detection, since they have higher speed and can traverse longer distances without much attenuation. This paper deals with the problem of

damage detection in thin aluminium alloy plates using Lamb wave propagation with lead zirconate titanate (PZT) wafers as transducers.

However, it is difficult to predict damage by monitoring changes from the baseline data, as the measured differences may be due to the large variation in structural dynamic characteristics that are caused by continuously changing operational and environmental conditions during the service life. This, along with the dispersive and multi-modal nature of Lamb wave propagation, results in significant technical difficulties in interpreting the signal changes between baseline and test data. To reduce the effects of dispersion of Lamb waves and to make the damage detection technique baseline free, researchers have been exploring the concept of time reversal [3, 4] for the last few years. According to the time reversibility of acoustics, an input signal can be reconstructed at the source point if an output signal recorded at another point is reversed in the time domain and emitted back to the same source point. The time reversal concept can be extended to Lamb wave propagation in order to detect defects in a thin

¹ Author to whom any correspondence should be addressed.

walled structure. The time reversibility property will not be preserved in the presence of damage in the wave path. There would be considerable difference between the input wave and the reconstructed wave obtained after time reversal.

Considerable research has been carried out to understand time reversibility since its observation in acoustics [5]. Subsequently the concept was extended to Lamb wave propagation [3, 4, 6–8] and the time reversibility of such waves has been studied extensively for its potential application to the development of baseline-free SHM schemes for damage detection. However, not much work on its actual use for damage detection has been reported in the literature, primarily due to the complexities associated with Lamb waves, including high wave speeds, the existence of multiple wave modes and the dispersive nature of the modes. The work reported in this paper was aimed at developing a damage detection scheme for metallic plates, through analysis of the reconstructed wave obtained experimentally.

Xu and Giurgiutiu [9] have studied single mode tuning effects on Lamb wave time reversal for damage detection. The trend of the experimental results presented shows that a combination of two modes, S_0 and A_0 , gives better reconstruction of the input signal by the time reversal process (TRP). Sohn *et al* [10] have studied the TRP for composite laminates and discussed that the original tone burst signal cannot be fully reconstructed because of frequency dependent attenuation referred to as amplitude dispersion [6]. Due to amplitude dispersion as well as the finite frequency band of the tone burst signal, the response signal is amplified non-uniformly which leads to the change of shape. In addition, Park *et al* [4] have shown the frequency dependence of the response amplitude by introducing the time reversal operator into the Lamb wave equation based on Mindlin plate theory. They also highlighted the significance of using a tone burst signal with narrower frequency band width. Sohn and Kim [11] have applied a damage detection algorithm to identify different types of damage. They have also shown the effects of different damage types on the time reversal of Lamb waves. Gangadharan *et al* [12] have shown that damage in metallic structures cannot be identified from the time reversibility of Lamb waves as these defects do not introduce any nonlinearity that breaks the TRP of Lamb waves and it is not possible to establish time reversal as a baseline-free technique for all structural damage types. In [12] the presence of damage is predicted by comparing the time reversed responses for damaged and undamaged structures. However, this is not a baseline-free technique.

In this paper, the damage detection is carried out using time reversibility of the Lamb waves in a thin aluminium plate with PZT wafers as transducers. A detailed experimental study has been carried out to understand the effects of excitation pulse frequency band width and transducer size on time reversibility. A set of criteria for selecting these parameters to achieve the best time reversibility has been proposed. The frequency dependence of the Lamb waves' response is investigated through experiments and a frequency region is suggested which minimizes the amplitude dispersion and improves the reconstruction of the original signal through TRP.

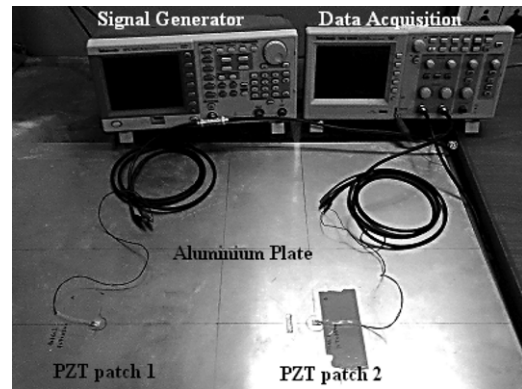


Figure 1. Picture of the experimental setup.

Next, experiments are performed by creating various kinds of damage in the aluminium plate to observe their effects on TRP. Through these experiments, it is shown that different kinds of damage in an isotropic plate can be detected using TRP and their effect on TRP can be quantified. Hence, it is possible to develop a baseline-free damage detection tool for structural health monitoring in isotropic thin plate like structures using the TRP of Lamb waves.

2. Experimental study of TRP

2.1. Experimental setup

The experimental setup consists of a Tektronix AFG 3021B signal generator and a Tektronix TDS 1002B digital storage oscilloscope, as shown in figure 1. The signal generator is used to generate a tone burst signal in the form of a sine wave modulated by different window functions. The Tektronix TDS 1002B digital storage oscilloscope is used for data acquisition of the response signals. The digital data are transferred to a computer for further offline processing. The plate specimen considered in the study is in the form of a 1.6 mm thick sheet of Al-5052 aluminium alloy (modulus of elasticity = 70.3 GPa, Poisson's ratio = 0.33, density = 2.68 g cm⁻³). The wafer-type PZT transducers (material type SP-5H) of different size from 5 mm square to 20 mm square with 0.5 mm thickness were used for actuation and sensing. They were bonded to the plate using a commercially available cyanoacrylate based adhesive.

The PZT patch transducers were bonded to the metallic plate (1250 mm × 1250 mm × 1.6 mm) with a separation of 290 mm to avoid mixing of the first two modes (S_0 and A_0) and the reflected waves from the specimen boundary. The Lamb waves were excited by one transducer and sensed by the second one. Figure 2(a) illustrates a typical input signal given to the PZT actuator and the corresponding response at the PZT sensor, at a central frequency of 200 kHz. The response shows the S_0 , A_0 modes and also the reflection from the edges, clearly separated.

Experiments have been carried out to identify the first two modes of Lamb wave propagation and for calculating the wave velocities of these modes at different central frequencies.

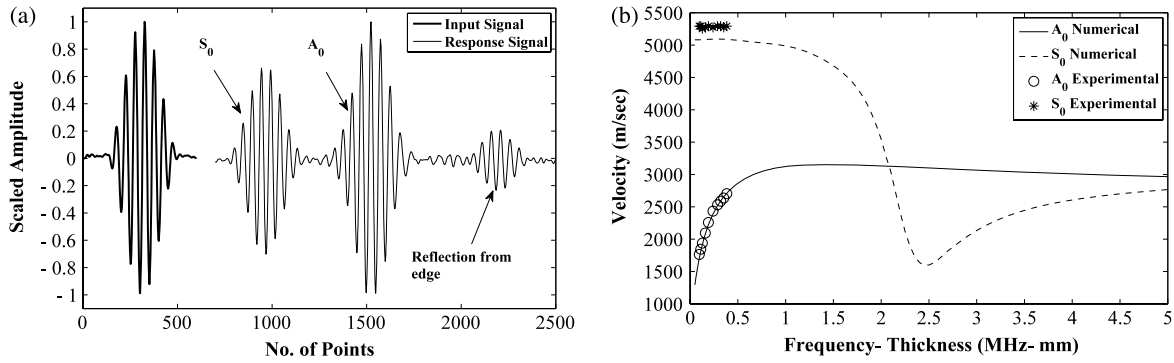


Figure 2. (a) Input and output signals and (b) experimental versus theoretical group velocities.

The experimental group velocities of A_0 and S_0 modes were calculated from the measured data and compared with those predicted computationally in figure 2(b). It can be seen that the theoretical and experimental velocities match well. For example, at 200 kHz the times of flight for S_0 and A_0 modes are $55.8 \mu\text{s}$ and $112.1 \mu\text{s}$ respectively and the distance travelled by the wave packet is 290 mm. Thus the group velocity at this frequency can be calculated as 5197 m s^{-1} for S_0 and 2587 m s^{-1} for A_0 . From the group velocity dispersion curves the corresponding theoretical velocities were obtained as 5082 and 2586 m s^{-1} , which are nearly equal to the respective experimental values.

As mentioned earlier, damage detection using Lamb waves involves several complexities and therefore the experiments need to be designed carefully. The wave and transducer parameters have to be selected so as to minimize the effect of two features, namely, dispersion and multi-modal wave propagation.

To reduce the effects of high frequency electro-magnetic noise, the recorded signals were filtered using a low-pass Butterworth filter. Further, the input signal and the reconstructed input signal are of different magnitude. Thus, to compare the shapes of input signals and the reconstructed input signals, all the signals were scaled to a magnitude of one by dividing the voltage values of all the data points of a signal by the maximum magnitude of that signal. Also, to alleviate the ill effects of dispersion and the presence of multiple modes in TRP, the effects of different parameters such as the tone burst signal frequency band width, the test frequency range and the size of the transducers were studied experimentally, as explained in the following subsections.

2.2. Signal frequency band width

It is important to have the best possible reconstruction of the input signal in order to detect the smallest effect of the damage on the TRP. It is necessary for the excitation to be of a narrow frequency bandwidth. This will result in less dispersion and hence in better reconstruction of the input signal during the TRP [3]. To generate a narrow band pulse we have used a modulated sinusoidal wave as the excitation signal. A number of modulation windows such as Gaussian, Morlet and Hanning windows were examined and it was observed that the

Table 1. The effect of the number of peaks on the signal bandwidth and TRP.

No. of cycles	4	5	7	8
Central frequency (kHz)	100	100	100	100
Frequency bandwidth (kHz)	54–146	64–136	73–127	76–124
% correlation	98.10	97.61	98.31	98.73
% root mean square deviation	21.86	23.12	16.81	13.60

Hanning window modulated tone burst signal gives a narrower frequency band compared to the others. Again, for a particular frequency, increasing the time length of the window yields a narrower frequency bandwidth but will create a longer time length pulse with more cycles, which will make it difficult to separate the different modes from the reflection. Thus, an optimal number of cycles has to be chosen while obtaining a narrower band of frequency. The effects of the number of cycles on TRP was studied experimentally. The results are presented as percentage correlation with original input signal.

Table 1 shows the correlation results for TRP conducted with a $10 \text{ mm} \times 10 \text{ mm} \times 0.8 \text{ mm}$ PZT transducer excited by a 100 kHz central frequency Hanning window tone burst signal with different numbers of cycles. The correlation formula used here to find out the similarity between the two data sets (reconstructed and original) is

$$r = \frac{S_{xy}}{S_x S_y} \quad (1)$$

where $S_x^2 = \frac{1}{n-1} \sum_{j=1}^n (x_j - \bar{x})^2$, $S_y^2 = \frac{1}{n-1} \sum_{j=1}^n (y_j - \bar{y})^2$, $S_{xy} = \frac{1}{n-1} \sum_{j=1}^n (x_j - \bar{x})(y_j - \bar{y})$, \bar{x} and \bar{y} are the mean values of the data sets, x_j and y_j respectively, n being the total number of data points in each set.

The similarity of two wave forms can also be analysed by calculating the error of reconstruction using the root mean square deviation calculation (RMSD) reported in [9].

$$\text{RMSD} = \sqrt{\frac{\sum_{j=1}^n (y_j - x_j)^2}{\sum_{j=1}^n x_j^2}} \quad (2)$$

The correlation coefficient is very sensitive to the phase change compared to amplitude variation. Hence the correlation coefficient will give a good estimation of the similarity of

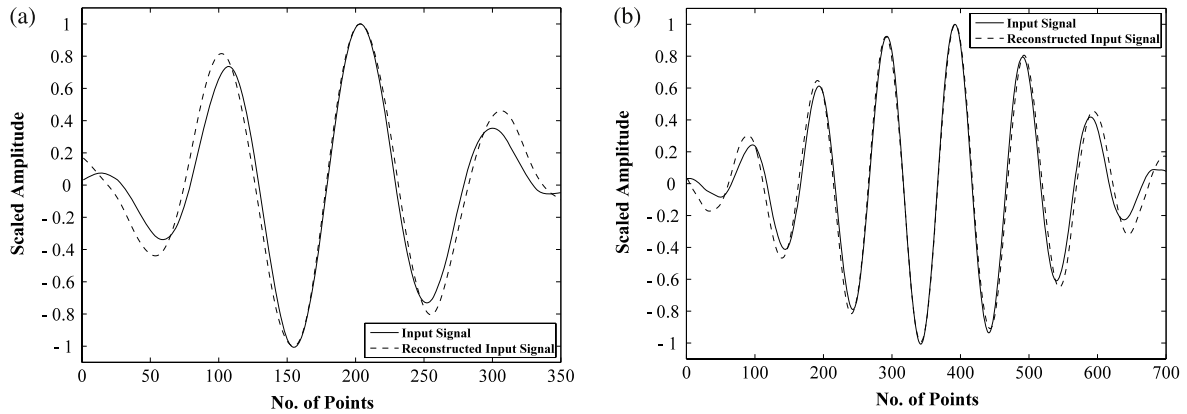


Figure 3. Reconstructed signal for (a) four peak and (b) eight peak Hanning window tone burst input signal.

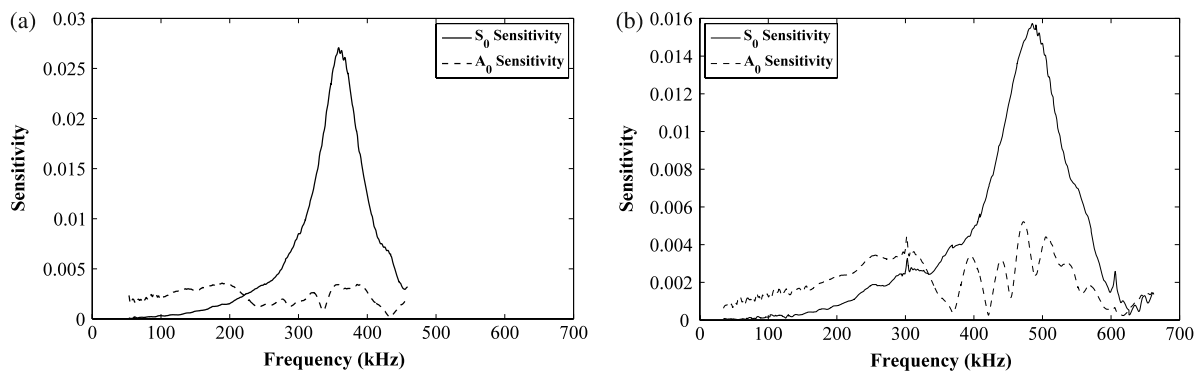


Figure 4. (a) Sensitivity variations for A_0 and S_0 mode with frequency for $7\text{ mm} \times 7\text{ mm} \times 0.5\text{ mm}$ and (b) sensitivity variations for A_0 and S_0 mode with frequency for $5\text{ mm} \times 5\text{ mm} \times 0.5\text{ mm}$.

two signals with respect to phase, whereas RMSD gives an estimation of the overall difference between two wave forms. It has been found, as shown later, that RMSD is not always a good measure over all cases of damage considered.

Figures 3(a) and (b) show the experimental result for TRP with different numbers of cycles in the tone bursts. It can be seen that better reconstruction is achieved using an eight-cycle Hanning window modulated tone burst signal. Keeping in mind the effect of cluttering with increasing the number of cycles, as mentioned before, the eight-cycle tone burst was selected for further experiments.

2.3. Test frequency

The frequency selection was done by considering the two types of dispersion as mentioned earlier, namely, velocity dispersion and amplitude dispersion. When the Lamb wave is actuated, due to finite frequency bandwidth, the different wave components corresponding to different frequencies travel at different velocities and therefore they reach the sensor at different times and a dispersed response is obtained. In the TRP, when the response signal at the sensor location is reversed in the time domain and sent back to the source location, the time reversed wave components, which are travelling at different speeds, reach the sensor location at the same time. Therefore velocity dispersion is minimized through the

TRP. However, due to the amplitude dispersion, the response signal at each step will be non-uniformly attenuated over the frequency band [6], which leads to changes in the shape from the original input even after normalization. Also, the velocity dispersion plot obtained by theoretical calculation and experimentation (figure 2(b)) shows that the phenomenon of velocity dispersion is well understood in theory. On the other hand, no experimental data on the dispersion of the excitation amplitude of a Lamb wave are available.

Therefore, the amplitude dispersion or dependency of the response amplitude on the frequency was studied here experimentally. The sensitivity plot showing the variation of amplitude response with the frequency of the Lamb wave was experimentally generated by calculating the ratios of magnitude of the FFT components of the input signal and the response signal at each frequency. Park *et al* [4] have investigated the TRP of a Lamb wave for a composite plate and a similar plot for the A_0 mode based on Mindlin plate theory was derived computationally. Figures 4(a) and (b) show such variation of amplitude ratio or sensitivity of S_0 and A_0 modes of an actuated Lamb wave with the frequency of actuation for 7 and 5 mm square PZTs. These plots were then used to minimize the effect of amplitude dispersion. To minimize the effect of amplitude dispersion one should perform experiments within a frequency band where the amplitude dispersion or sensitivity variation is small. Here, the range of frequency

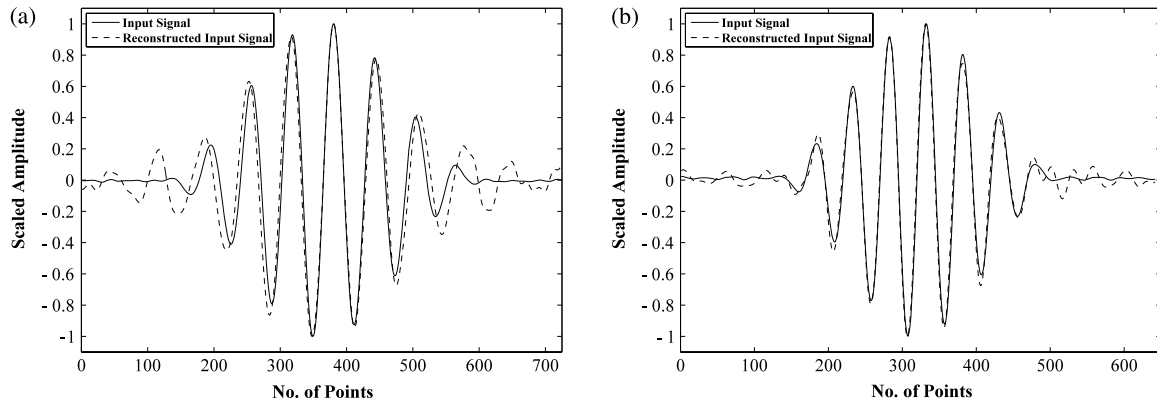


Figure 5. Reconstruction at (a) 40 kHz and (b) 200 kHz.

Table 2. Similarity analysis for reconstructed input signal and original input signal.

Central frequency (kHz)	Frequency band (kHz)	% correlation	% RMSD
40	30.4–49.6	95.83	30.22
60	45.6–74.4	98.6	19.86
80	60.8–99.2	98.49	17.51
100	76–124	98.82	15.65
120	91.2–148.8	99.71	9.34
150	114–186	99.51	10.13
180	136.8–223.2	98.72	18.33
200	152–248	99.59	9.07
220	167.2–387.2	94.18	36

Table 3. Similarity analysis for the reconstructed signal and original input signal with different patch size.

Frequency (kHz)	5 mm patch		7 mm patch	
	% Correlation	RMSD	% Correlation	RMSD
40	98.53	19.28	95.83	30.22
60	98.69	16.5	98.6	19.86
80	98.38	18.66	98.49	17.51
100	99.03	16.26	98.82	15.65
120	98.94	11.98	99.71	9.34
150	98.93	16.19	99.51	10.13
180	98.84	15.81	98.72	18.33
200	97.76	21.7	99.59	9.07
240	96.8	27.83	94.95	31.59

for experiments using 7 mm square PZT is selected as 40–250 kHz, as within this band the amplitude dispersion of S_0 and A_0 is low (see figure 4(a)). From these figures it is also noteworthy that the amplitude dispersion varies with the size of PZT. This variation with PZT size can be attributed to the spatial distribution of the actuation. Another important point is the variation of sensitivity of A_0 with frequency, which suggests that it is sensitive to parameters other than the frequency of excitation. One such parameter could be the bonding between PZT patches and the plate surface [13]. This, however, should be investigated in detail through modelling of the PZT transducers bonded on the plate.

To further optimize the reconstructed signal, experiments were carried out at different frequencies ranging between the 40 and 220 kHz band for the PZT transducer size of a 7 mm square. The correlation coefficients and RMSD values are tabulated in table 2. The maximum correlation is achieved at a frequency of 120 kHz. The correlation is about the same at 150 and 200 kHz, all values being above 99.5%, whereas at 200 kHz RMSD is lowest. Amongst these the test frequency for the damage detection is thus decided as 200 kHz, since the shorter wavelength is better to predict smaller size damage.

Figure 5(a) shows the experimental data for the time reversed reconstructed input signal with original input at 40 kHz and figure 5(b) shows the experimental data for the time reversed reconstructed input signal with original input at 200 kHz. It can be seen that a better reconstruction is observed at 200 kHz as shown by the correlation given in table 2.

2.4. Transducer size

The criterion to select the transducer size is to obtain the highest possible actuation at a particular frequency to get a good signal to noise ratio. Giurgiutiu [14] studied Lamb waves in plates and found that for a particular frequency best actuation of a Lamb wave can be achieved by selecting a PZT wafer length to be about half the wavelength of a particular Lamb wave mode. Therefore it is important to investigate the effect of transducer size on the time reversal process also. It is, however, difficult to optimize the transducer size based on this theory where both S_0 and A_0 are getting excited simultaneously. Therefore, for multi-modal actuation of the Lamb wave, it is necessary to study the variation of actuation with the size of PZT, experimentally. Also the size of PZT affects the phenomenon of amplitude dispersion (figures 4(a) and (b)) which affects the quality of reconstruction of the input signal. Therefore, it is necessary to study the effect of different sizes of PZT for actuation of Lamb waves at different frequencies on TRP.

The similarity indices for a 5 mm square and 7 mm square patch at different excitation frequencies are presented in table 3. It is found that the maximum similarity can be achieved at different frequencies for different sizes of transducers. For example, at a frequency of 100 kHz a 5 mm patch gives better similarity than a 7 mm patch. In contrast, a 7 mm patch is advisable for a frequency of 120 kHz. This is a corollary of the earlier observation from figures 4(a) and (b).

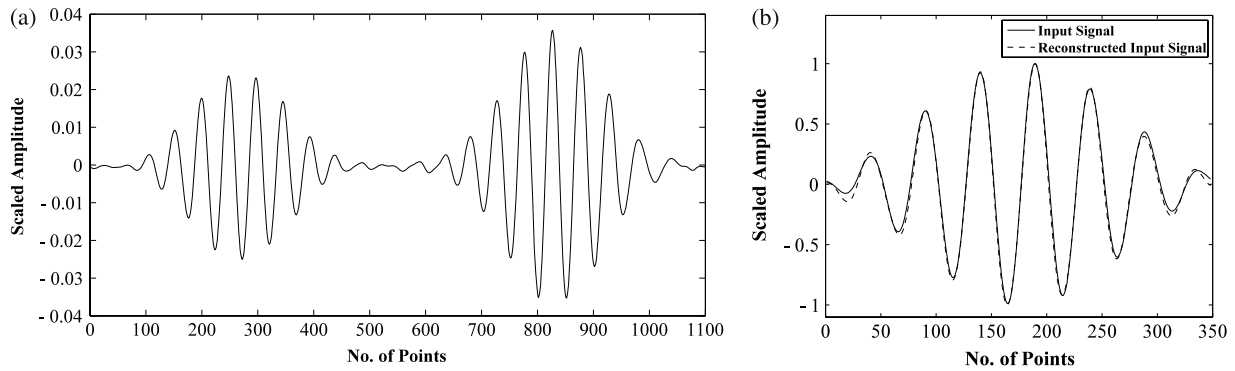


Figure 6. (a) The forward wave recorded at the sensor (undamaged) and (b) the reconstructed input wave (undamaged) compared with the input signal.

From table 3 it is found that a 7 mm PZT gives better reconstruction in TRP than a 5 mm PZT in most cases. Therefore a 7 mm PZT is chosen for the damage detection experiments.

3. Damage detection using TRP

In the TRP the Lamb wave travels twice through the damage. Thus the damage affects the wave packet twice; first in the forward path and second in the time reversed path. Hence it is expected that the TRP, compared to other Lamb wave based methods should be sensitive to much smaller damage. To detect small effects of damage on the TRP it is important to first have a good reconstruction of the input signal in an undamaged plate. The choice of experimental parameters to obtain the best reconstruction has been discussed in the earlier sections. The comprehensive experimental study carried out has enabled good reconstruction for undamaged structures. In this section, the experiments performed to detect various kinds of representative damage in an isotropic plate are reported. The experiments are performed on the same plate structure with various types of artificial damage, to study the effect of the damage on the time reversibility of a Lamb wave. In addition, in the present work, the suitability of using the TRP as a baseline-free damage detection scheme is emphasized. This is in contrast to the earlier works on the TRP based damage detection where information about the undamaged structure is also used [12]. In the other reported work [10], the effect of damage on the TRP has only been discussed through theoretical analysis. Here, the representative artificial damages are studied using a block mass in the form of a 22 mm diameter, 3 mm thick metallic coin pasted between the sensor and actuator, a notch of length 25 mm, width 2 mm and depth 0.8 mm, and a 0.8 mm thick, rectangular surface erosion of length 25 mm and width 7 mm. The results are given in figures 6–9.

In figure 6, which corresponds to the case of an undamaged plate, it can be seen that in the forward signal the S_0 and A_0 modes are clearly separated and it can be seen that the input wave is well reconstructed by time reversal. From figures 7 to 9, it is seen that the various types of damage affect the forward signal of the Lamb wave propagation in different

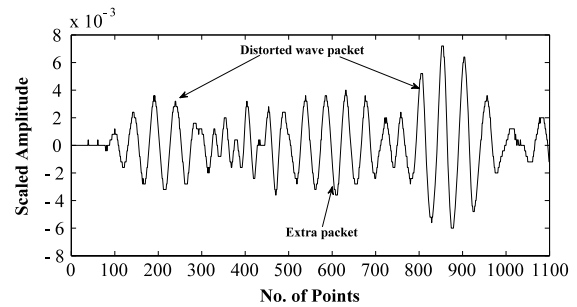


Figure 7. The forward wave recorded at the sensor (with the coin).

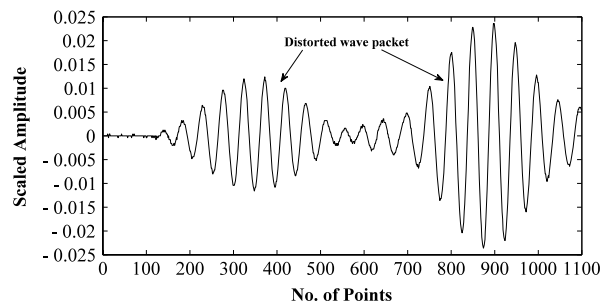


Figure 8. The forward wave recorded at the sensor (with the notch).

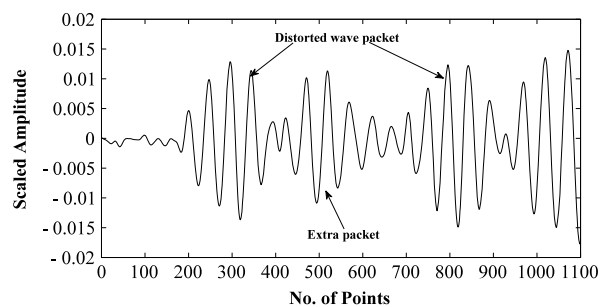


Figure 9. The forward wave recorded at the sensor (with the surface removed).

fashions. It can be seen from figure 7 that in the case of the coin placement there is an extra packet between S_0 and A_0 which may distort the reconstructed signal in time reversal. Similarly,



Figure 10. The metallic coin at 145 mm from actuator.

figure 8 shows the case of the notch and here the wave packets of S_0 and A_0 are distorted and appear elongated. Figure 9 shows the forward response for the case of surface removal. Here the wave packets are distorted as well as an extra packet appearing between S_0 and A_0 . In the following subsections, the effect of the damage on the reconstructed signal is studied in detail.

3.1. Experiment using a metallic coin

In this experiment, as discussed earlier, a metallic coin of 22 mm diameter and thickness of 3 mm was placed at distances 33 mm, 145 mm (figure 10) and 257 mm from the actuator and the patches were excited with eight cycles of a tone burst signal using a Hanning window at 200 kHz central frequency. The two patches were placed at 290 mm from each other.

Figures 11(b), 12(a) and (b) present the input and reconstructed signals for the undamaged case and the three positions of the coin, namely, 33, 145 and 257 mm from the actuator as explained before. Table 4 gives the similarity in terms of correlations and RMSDs for all the three cases. From figures 11 and 12 and table 4 it is clear that a coin placed in

Table 4. Similarity between the reconstructed input signal and the input signal (with coin).

	% correlation	% RMSD
Undamaged	99.59	9.07
Coin at 257 mm from actuator and 33 mm from sensor	88.78	46.44
Coin at 145 mm from both sensor and actuator	63.50	90.93
Coin at 33 mm from actuator and 257 mm from sensor	6.69	136.27

between the sensor and actuator is easily detectable using time reversal of the Lamb wave without using any baseline data. It can also be seen that the correlation in the reconstruction varies with the position of the coin. The correlation is a minimum when the coin is close to the actuator and is better when it is away from the actuator. It can be seen that the correlation in reconstruction is significantly lower even when the coin is placed close to the sensor compared to a 99.59% correlation without any coin. Thus the coin is detectable without any baseline data for all the three positions.

3.2. Experiment with notch

In this experiment a 0.8 mm deep, 3 mm wide and 26 mm long notch was created between the sensor and actuator which were placed 290 mm apart from each other. The notch was created

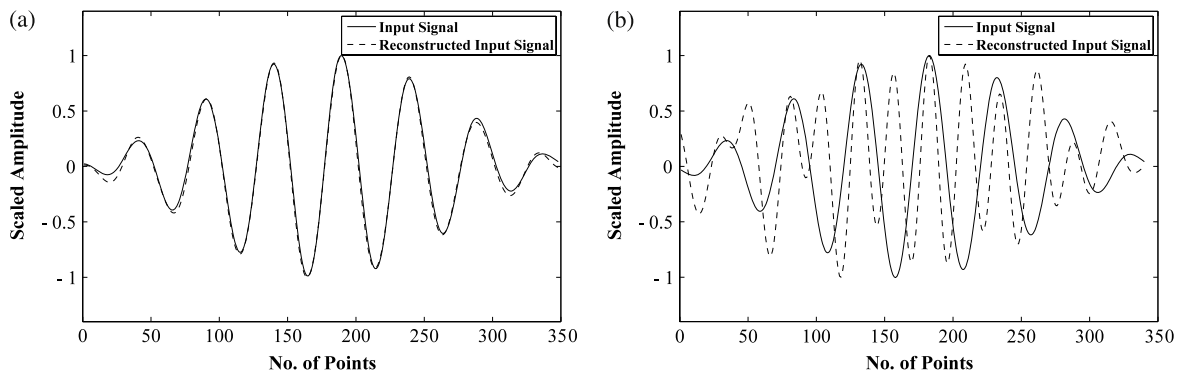


Figure 11. (a) The reconstructed input signal and original input signal (without coin) and (b) the reconstructed input signal and original input signal (coin at 33 mm from the actuator).

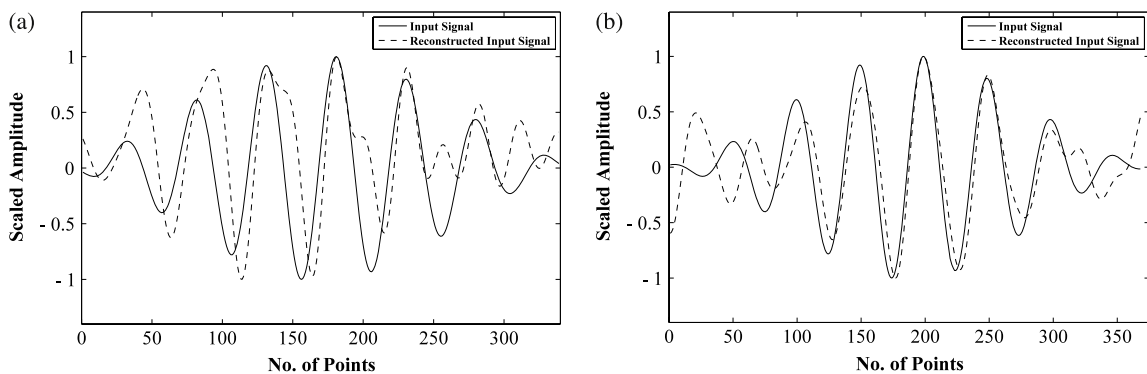


Figure 12. (a) The reconstructed input signal and original input signal (coin at 145 mm from the actuator) and (b) the reconstructed input signal and original input signal (coin at 257 mm from the actuator).



Figure 13. The notch at 65 mm from the actuator.

at 65 mm from the PZT patch B (the patch at the left side of figure 13) and the patches were excited with eight cycles of a tone burst signal using a Hanning window at 200 kHz central frequency. In the first case patch B was actuated making patch A (the patch at the right side of figure 13) the sensor and in the second case patch A was actuated with patch B used as sensor.

Figure 14(a) present the reconstructed signal for the notch placed at 225 mm from the actuator. Table 5 gives the similarity in terms of correlations and RMSDs for the two cases namely, with the notch present at 65 and 225 mm from the actuator. From figures 14(a) and table 5, it is observed that in both cases the %RMSD in reconstruction is much higher for the notched plate compared to the %RMSD in the case of the undamaged plate. Although the difference does not vary much with the distance of the damage from the actuator, in contrast to the observations in the experiments performed with the coin, it is easily detectable with the TRP of the Lamb wave, irrespective of the distance. The correlation in reconstruction drops to lower values in the range of 97%–94%. Along with this, if one compares figure 12(b) with figure 14(a), it can be seen that, fundamentally, the forms of distortions are different in the case of the notch and block mass. In the case of the block mass the reconstructed wave is different from the input signal both in phase and amplitude and extra cycles also have appeared at the beginning and end of the reconstructed wave packet, whereas in the case of the notch the reconstructed signal is different from the input signal in amplitude with little change in phase. Also, it appears that the reconstructed packets have simply been elongated with more cycles, as shown in figure 14(b). It can be seen that in the case of the attached block mass (figure 7), the forward signal shows the presence of an extra wave packet between S_0 and A_0 , distorting both the phase and magnitude of the reconstructed wave and introducing extra cycles at the beginning and the end of the reconstructed wave packet. Whereas, due to the presence of the notch, in the forward signal shown in figure 8, the two wave packets of S_0 and A_0 have elongated with more cycles without much change



Figure 15. Surface damage at 32 mm from the actuator.

Table 5. Similarity between the reconstructed input signal and the input signal (with the notch).

	% Correlation	% RMSD
Undamaged	98.19	20.00
Notch at 225 mm from actuator	96.50	33.72
Notch at 65 mm from actuator	94.27	40.96

in phase. Thus the same effect can be seen in the reconstructed signal.

3.3. Experiment with surface damage

In this experiment material was removed to a depth of roughly 0.8 mm from a 7 mm wide and 26 mm long area of the plate between the sensor and actuator placed 270 mm apart. The damage was located at 32 mm from the PZT patch B (the patch at the left side of figure 15). As before, the actuator patch was excited with eight cycles of a tone burst signal using a Hanning window at 200 kHz central frequency. In the first case patch B was actuated making patch A (the patch at the right side of figure 15) the sensor and in the second case patch A was actuated with patch B used as the sensor.

Figure 14(b) presents the input and reconstructed signals for the case of the surface damage present at 238 mm from the actuator and table 6 gives the similarity in terms of correlations and RMSDs for the two cases. From figure 14(b) and table 6, it is observed that in both cases of surface damage, the difference in the reconstruction is much higher than the case of the undamaged plate. The %RMSD in reconstruction varied within 24%–80% due to the presence of surface damage. Therefore, surface damage can easily be detected using the TRP of a Lamb wave as the presence of the damage increases the error in the reconstruction from 8% to a high value of 80% with significant decrease in correlation factor.

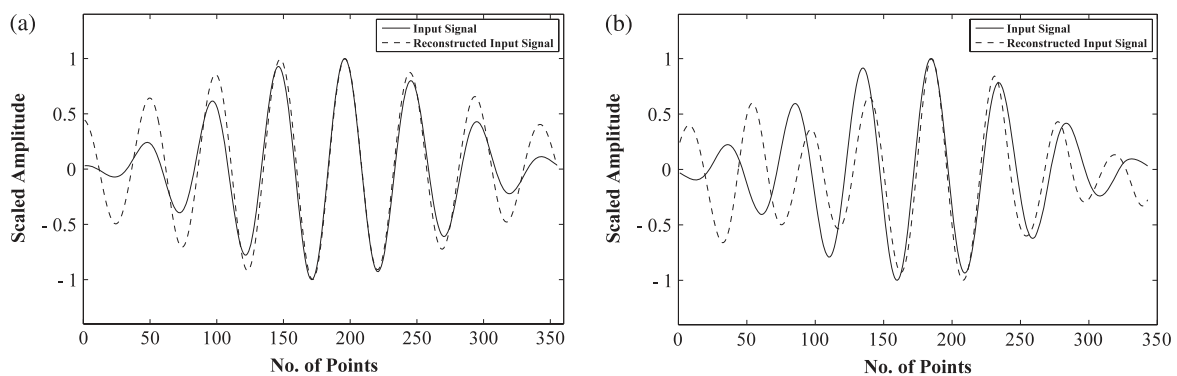


Figure 14. (a) The reconstructed input signal and original input signal (with the notch at 225 mm from the actuator) and (b) the reconstructed input signal and original input signal (with surface damage at 238 mm from the actuator).

Table 6. Similarity between the reconstructed input signal and the input signal (with surface damage).

	% Correlation	% RMSD
Undamaged	99.68	7.97
Damage at 32 mm from actuator	97.28	24.10
Damage at 238 mm from actuator	67.50	79.94

From these experimental results, comparing figures 12(b) and 14(b) it can be observed that the two types of damage, namely, surface removal and the attached block mass affect the reconstructed signal in a similar pattern. In both cases the damage was placed relatively far from the actuator and closer to the sensor and in both cases the distortions of the reconstructed signals are similar. This can be explained by comparing figures 7(a) and 9(a). These figures show that the effects of the two types of damage on the forward signals are similar. In both cases an extra packet appeared between S_0 and A_0 due to the presence of damage. In both cases this extra packet distorts the reconstructed wave both in phase and in amplitude and also introduces extra cycles at the beginning and end of the reconstructed wave packet. These preliminary observations suggest that a block mass attached to the surface of the plate and some material removed from the surface of the plate could have a similar effect on the propagation of the Lamb wave, both essentially giving rise to a step change in plate thickness over the area of the damage. Further experimental investigation is required to confirm these observations.

In table 5 it is observed that in the case of the undamaged plate a minor change of phase in the reconstructed signal results in a considerable RMSD value of 20% without significant distortion of shape and with a high correlation value of above 98%. On the other hand, in table 6 in the case of damage at 32 mm from the actuator, the RMSD value is 24% with significant distortion of shape. This implies to us that although RMSD is a useful preliminary tool for comparing the input and reconstructed signals for damage detection, it cannot distinguish distortion of signal shape due to damage from minor phase shift of the reconstructed input signal due to experimental variations. The correlation value evolved in this paper, however, is a much more reliable measure for damage prediction. Also, the use of other better measures to identify distortion of signal shape may result in a more confident prediction of damage.

4. Conclusion

An experimental study has been presented to explore the suitability of time reversibility of a Lamb wave for baseline-free damage detection in a metallic plate. The experiments were carried on an aluminium plate using PZT wafers as transducers to generate and detect Lamb wave responses. The experimental results were first validated by comparing the A_0 and S_0 mode velocities obtained experimentally with the theoretically calculated dispersion plot.

A series of experiments were performed first to understand the time reversibility of the Lamb wave. The effect of tone burst signal frequency band width on time reversibility was

studied experimentally on the basis of quality of reconstruction and it was found that a tone burst signal with more cycles gives better reconstruction as the frequency band becomes narrower with a greater number of cycles.

From the velocity dispersion plot it is expected that the desirable band of frequency of actuation is where there is least velocity dispersion in both S_0 and A_0 . The quality of reconstruction, however, depends heavily on the amplitude dispersion as time reversibility minimizes the effects of velocity dispersion but cannot reduce the effect of amplitude dispersion. It was shown that in TRP the quality of reconstruction depends, to a large extent, on the selection of the frequency bandwidth which controls the amplitude dispersion. In addition, the dependence is much less upon velocity dispersion and more upon amplitude dispersion.

It was observed from the experiments that the amplitude dispersion depends on the actuator size. Therefore, for each actuator, the amplitude dispersion plot would suggest the range of frequencies that should give better reconstruction. Thus it is concluded that the proper size of transducer selection is also very important. Based on these two parameters, a frequency can be selected to obtain a good reconstruction. This is important as better reconstruction of input signal increases the possibility of detecting damage which has a small effect on the TRP.

In the other set of experiments, it was observed that the presence of surface damage can be detected by quantifying the reconstruction. It was observed that significant distortion in the reconstructed input signal occurred in the case of a block mass attached to the surface of the plate. This distortion of the reconstructed signal can be quantified by comparing it with the input signal and could be used as a basic form of damage detection tool. In the second experiment, it was observed that the TRP is able to capture the presence of a notch in the path of wave propagation and the effect of the notch on the Lamb wave is different from the effect of a block mass. The presence of surface erosion also affects the TRP in a way similar to that of an attached block mass and is easily detectable.

The experimental study with various kinds of damage shows that it is possible to detect the presence of different kinds of damage in the wave propagation path in a metallic plate without using baseline data, but using the time reversibility of a Lamb wave. These results show the promise of TRP in developing a baseline-free damage detection tool.

References

- [1] Farrar C R and Worden K 2007 An introduction to structural health monitoring *Phil. Trans. R. Soc. A* **365** 299–301
- [2] Chang F K (ed) 2005 *Structural Health Monitoring 2005: Advancements and Challenges for Implementation* (Lancaster, PA: Destech Publications)
- [3] Ing R K and Fink M 1998 Time-reversed Lamb waves *IEEE Trans. Ultrason. Ferroelectr. Freq. Control* **45** 1032–43
- [4] Park H W, Sohn H, Law K H and Farrar C R 2007 Time reversal active sensing for health monitoring of a composite plate *J. Sound Vib.* **302** 50–66
- [5] Fink M 1999 Time-reversed acoustics *Sci. Am.* **281** 91–7
- [6] Park H W, Kim S B and Sohn H 2009 Understanding a time reversal process in Lamb wave propagation *Wave Motion* **46** 451–67

- [7] Jha R and Watking R 2009 Lamb wave based diagnostics of Composite plates using a modified time reversal method *50th AIAA/ASME/ASCE/AHS/ASC Structures, Structural Dynamics, and Materials Conf. (Palm Springs, CA)*
- [8] Lee S J, Sohn H and Hong J W 2010 Time reversal based piezoelectric transducer self diagnosis under varying temperature *J. Nondestruct. Eval.* **29** 75–91
- [9] Xu B and Giurgiutiu V 2007 Single mode tuning effects on Lamb wave time reversal with piezoelectric wafer active sensors for structural health monitoring *J. Nondestruct. Eval.* **26** 123–34
- [10] Sohn H, Park H W, Law K H and Farrar C R 2007 Damage detection in composite plates by using an enhanced time reversal method *J. Aerosp. Eng.* **20** 141–51
- [11] Sohn H and Kim S 2009 Methods apparatuses and systems for damage detection *US Patent Publication Pub. No. US 2009/03011 98 A1 Pub.* 10 Dec 2009
- [12] Gangadharan R, Murthy C R L, Gopalakrishnan S and Bhat M R 2009 Time reversal technique for health monitoring of metallic structure using Lamb waves *J. Ultrason.* **49** 696–705
- [13] Nieuwenhuis Jeroen H, Neumann John J Jr, Greve David W and Oppenheim Irving J 2005 Generation and detection of guided waves using PZT wafer transducers *IEEE Trans. Ultrason. Ferroelectr. Freq. Control* **52** 2103–11
- [14] Giurgiutiu V 2003 Lamb wave generation with piezoelectric wafer active sensors for structural health monitoring *10th Int. Symp. on Smart Structures and Materials; Proc. SPIE* **5056** 111–22